14TH CANADIAN MASONRY SYMPOSIUM
MONTREAL, CANADA
MAY 16TH – MAY 20TH, 2021

AN ANALYTICAL MODEL FOR SHEAR-DOMINATED PARTIALLY GROUTED REINFORCED MASONRY SHEAR WALLS

Al-Ahdal, Abdulelah[1]; Aly, Nader[2] and Galal, Khaled[3]

ABSTRACT

Although many studies have been conducted on reinforced masonry shear walls since the mid of the last century, those concerned with partially grouted (PG) reinforced masonry shear walls are limited. Moreover, load-displacement analytical models for PG walls are scarce. Therefore, developing simplified analytical models that can predict the behaviour of these walls is essential. In the current study, an analytical load-displacement backbone model is proposed for shear-dominated PG masonry shear walls. Due to the limited experimental data and the absence of enough data points for the analytical model, a matrix of numerical models was established to cover a wide range of parameters. The nonlinear finite element model was validated against several experimental specimens from the literature. The parameters covered by the numerical model included aspect ratio, spacing between vertical and horizontal grouted cells, axial load, ratio of vertical and horizontal reinforcement, and compressive strength of grouted and ungrouted masonry units. The analytical model is defined by five points: cracking, yielding, ultimate, 20% strength degradation, and 40% strength degradation. The fifth point was essential as it was reported in previous experimental results that there is a significant degradation in the strength immediately after ultimate load. The analytical model was calibrated against a total of 65 shear-dominated PG walls, 3 specimens from the existing experimental database and 62 specimens generated from the numerical model. The results show that the proposed analytical model provides a good prediction of the lateral load-displacement backbone of shear-dominated PG masonry walls.

KEYWORDS: *masonry, partially grouted, backbone, shear-dominated, numerical analysis, analytical model*

[1] Ph.D. student, Department of Building, Civil and Environmental Engineering, Concordia University, 1515 St. Catherine West, Montreal, QC, Canada, abdulelah.al-ahdal@concordia.ca

[2] Owner's Engineering Lead, Bruce Power, ON, Canada. Formerly, Postdoctoral Fellow, Department of Building, Civil and Environmental Engineering, Concordia University, 1515 St. Catherine West, Montreal, QC, Canada, Nader.essam.aly@gmail.com

[3] Professor, Department of Building, Civil and Environmental Engineering, Concordia University, 1515 St. Catherine West, Montreal, QC, Canada, khaled.galal@concordia.ca

INTRODUCTION

Partially grouted (PG) masonry walls have narrow limitations in the current building codes to be used as seismic-resistant structural elements even though some post-earthquake inspections reported that many of these types of walls did not experience a complete collapse in significant earthquakes such as the 2010 Maule and the 2014 coast of Iquique earthquakes [1,2]. Additionally, recent studies proposed various adjustments for PG walls such as using double-cells instead of single-cell grouting for both vertical cells and bond beams and using bed-joint reinforcement in addition to bond beam reinforcement to improve their performance and ductility [3–7]. Therefore, while PG walls' behaviour is more complex and less predictable than that of fully grouted (FG) walls, some detailing enhancements can be applied to this type of wall to produce more efficient, more economical, and less materials-consuming structural elements.

Although various experimental studies have been conducted in recent decades to evaluate the PG walls' in- and out-of-plane response, most of them concentrated on their shear behaviour. PG masonry walls are only used with limited heights, i.e., low-rise buildings, which makes the flexural-dominated PG masonry walls missing from the literature. To fill this gap, numerical and analytical models were generated to study PG masonry walls' local and global behaviours. Numerical modeling of PG walls has remarkable limitations in the research environment due to its intricacy. On the other hand, simplified analytical (backbone) models are preferred by practicing engineers due to their ease of application. These models are usually derived from extensive data based on statistical analysis to produce more simplified expressions that can be used in engineering practice. More recent analytical models were developed to simulate and predict the behaviour of reinforced masonry shear walls (RMSWs) [8–12]; however, these models were only validated against FG masonry walls and seem to be inapplicable to PG masonry walls. Therefore, developing analytical models that describe PG masonry shear walls' behaviour becomes essential and, with an equal degree, challenging.

An extensive analytical analysis was executed in the present study to create a simplified backbone model that predict the response of shear-dominated PG masonry shear walls based on a nonlinear finite element (FE) numerical model. This numerical model is employed to generate a comprehensive matrix to compensate for the experimental data shortage. Finally, this matrix in addition to accessible experimental data are utilized to explicitly establish new analytical models for PG masonry shear walls using regression analysis.

NUMERICAL MODEL

Due to the limitation in the experimental database, a numerical model is necessary to be developed. Modeling of masonry structures is confined within three main approaches that have been used widely in literature: macro models, micro models, and simplified-micro models [13]. In the current study, the 2D simplified-micro modeling using ABAQUS/Expl-icit has been adopted, as shown in Figure 1. Grouted and ungrouted cells were modeled as solid elements with thicknesses of the concrete block and the face shells, respectively, while the reinforcement was modeled as a onedimensional truss element. The mortar was not physically modeled; however, its properties have been defined using the cohesive element modeling through surface contact. For materials definition, the uniaxial concrete model proposed by Hsu and Hsu [14] for concrete was utilized for the grouted units while the uniaxial compressive and tensile stress-strain relationships of masonry proposed by Ewing et al. [15] are employed for ungrouted units. Finally, the exact, experimentally obtained stress-strain curves of the reinforcement were defined.

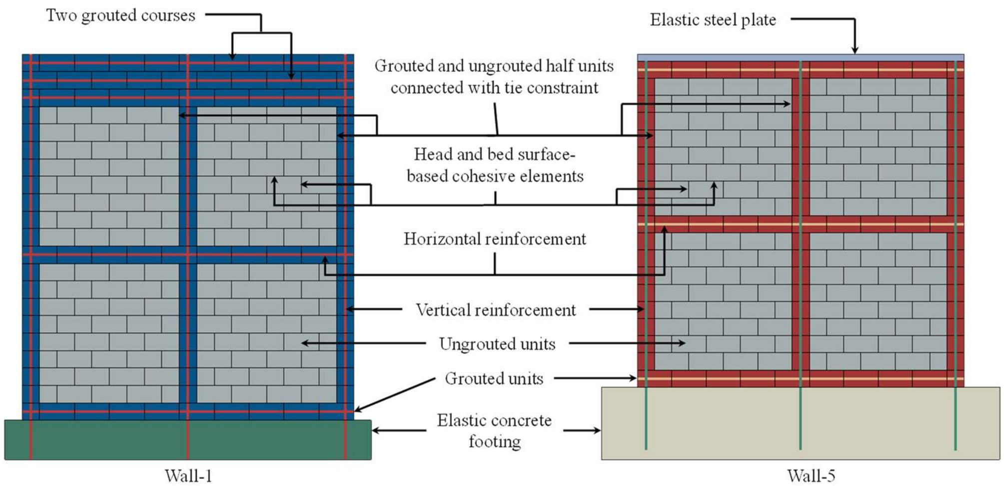

Figure 1: Finite Element Model Using ABAQUS

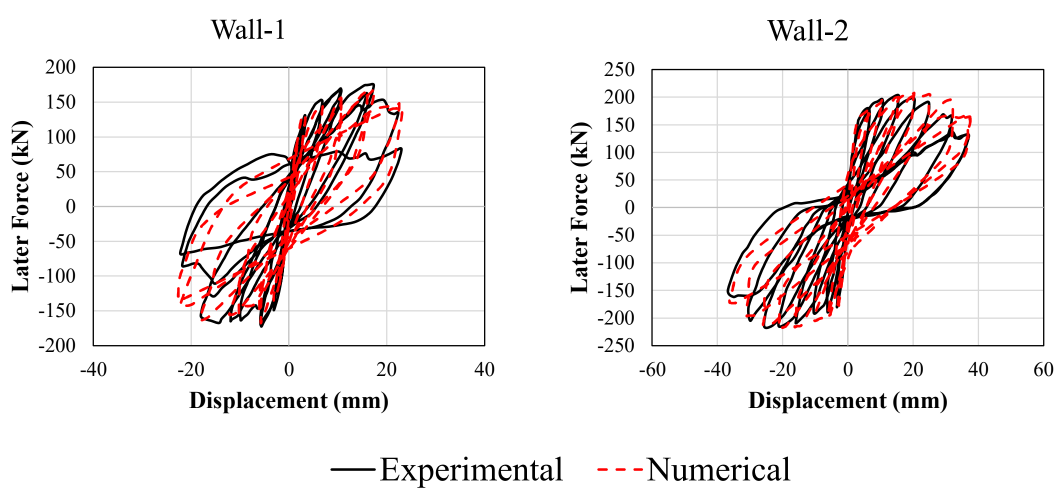

Figure 2: Samples of Numerical Model Validation

The model has been validated against eight experimental specimens by Bolhassani [5] and Malek [16], and the results showed a good agreement with the experimental outputs. Figure 2 shows the hysteric behavior of two samples (Wall-1 and Wall-2). As can be seen, the numerical model could capture the initial stiffness, the yielding point, and the peak capacity. Moreover, the model was able to simulate the hysteretic response of the PG masonry shear walls.

Table 1: Matrix of Numerical Models.

Aspect ratio	Wall ID	Reinforcement Ratios*		Grouted Comp. Strength (MPa)	Ungrouted Comp. Strength (MPa)	Axial Stress* (MPa)
		Vertical (%)	Horizontal (%)			
1.74	01 – 02	0.308	0.034, 0.021	12.43	21.61	0.75
	03 – 04	0.432, 0.308	0.041, 0.28	12.43	21.61, 18	0.75
1.63	05 – 06	0.308	0.029, 0.022	12.43	21.61	0.75
	07 – 09	0.432, 0.308	0.044, 0.039, 0.029	12.43	21.61, 18	0.75
1.48	10	0.308	0.032	12.43	21.61	0.75
	11 – 14	0.432, 0.308	0.32, 0.49, 0.43, 0.24	12.43	21.61, 18	0.75, 1.25
1.32	15 – 19	0.308, 0.176	0.064, 0.045, 0.036, 0.027	12.43	21.61	0.75
	20 – 26	0.308, 0.176, 0.132, 0.432	0.064, 0.045, 0.048, 0.027	12.43	21.61, 18	0.75, 1.25
1.11	27 – 32	0.308, 0.176, 0.132	0.065, 0.054, 0.032	12.43	21.61	0.75
	33 – 46	0.308, 0.176, 0.132, 0.432, 0.247, 0.185	0.087, 0.065, 0.043, 0.032	12.43, 15	21.61, 18	0.25, 0.75, 1.25
1.0	47 – 51	0.308, 0.176, 0.132	0.084, 0.048, 0.036	12.43	21.61	0.75
	52 – 62	0.308, 0.176, 0.132, 0.432, 0.247	0.084, 0.036, 0.048	12.43, 15	21.61, 18	0.25, 0.75, 1.25
	Wall-1**	0.19	0.05	12.43	21.61	0.75
	Wall-2**	0.18	0.05	12.43	21.61	0.75
	Wall-3**	0.16	0.05	12.43	21.61	0.75

*Based on gross area.
**Experimental specimens tested by Maleki [16]

ANALYTICAL MODEL

Database of Numerical Models

A total of 65 PG masonry shear walls, presented in Table 1, were established as a database for developing the analytical backbone model for shear-dominated PG masonry walls. Three walls were experimentally tested by Maleki [16] while the remaining 62 specimens were numerically generated for aspect ratios ranging between 1.0 and 1.75. Fixed wall length limited the number of vertical spacing to only three spacings of 285, 570, and 855 mm between grouted cells, while varied heights permit extending the matrix by increasing the number of bond beam spacings. In addition to the horizontal and vertical spacing parameters, different bar diameters were employed to expand the covered area of vertical and horizontal reinforcement ratios. Furthermore, three constant axial stresses of 0.25, 0.75, and 1.25 MPa were applied on walls alternatively to investigate the effect of axial load on the walls' behaviour. Finally, the compressive strengths of grouted and ungrouted masonry of the original experimental study by Maleki [16] were used with an approximate extension of ± 20% to duplicate the walls.

Evaluation of Previous Analytical Models for PG Walls

Several analytical models have been developed to describe the behaviour of masonry structures. Specifically, four backbone models [9,11,12,17] were generated to predict RMSWs response in terms of several performance points, however; most of these models were calibrated and validated against FG walls. In this section, these analytical models are tested against random samples of the established matrix of the numerical models (walls 05, 13, and 16) to investigate their validity against PG masonry walls. Although, walls 05, 13, and 16 were selected randomly, they were distributed to cover different parameters. These walls were intentionally selected to have different aspect ratios of 1.63, 1.48, and1.32, respectively. Moreover, they have similar vertical reinforcement ratio of 0.308 but different horizontal reinforcement ratios of 0.029, 0.043, and 0.045, respectively.

As can be seen in Figure 3, the available models, [9,11,12,17], cannot accurately describe the behaviour of PG walls. All models overestimate the initial stiffness of PG masonry walls since they consider the gross stiffness before cracking. Moreover, ASCE 41-17 and Ezzeldin et. al. models, [11,17], overestimate the post-peak behaviour and predict failure at higher displacement values. Thus, developing simplified analytical models specialized for PG masonry shear walls is essential.

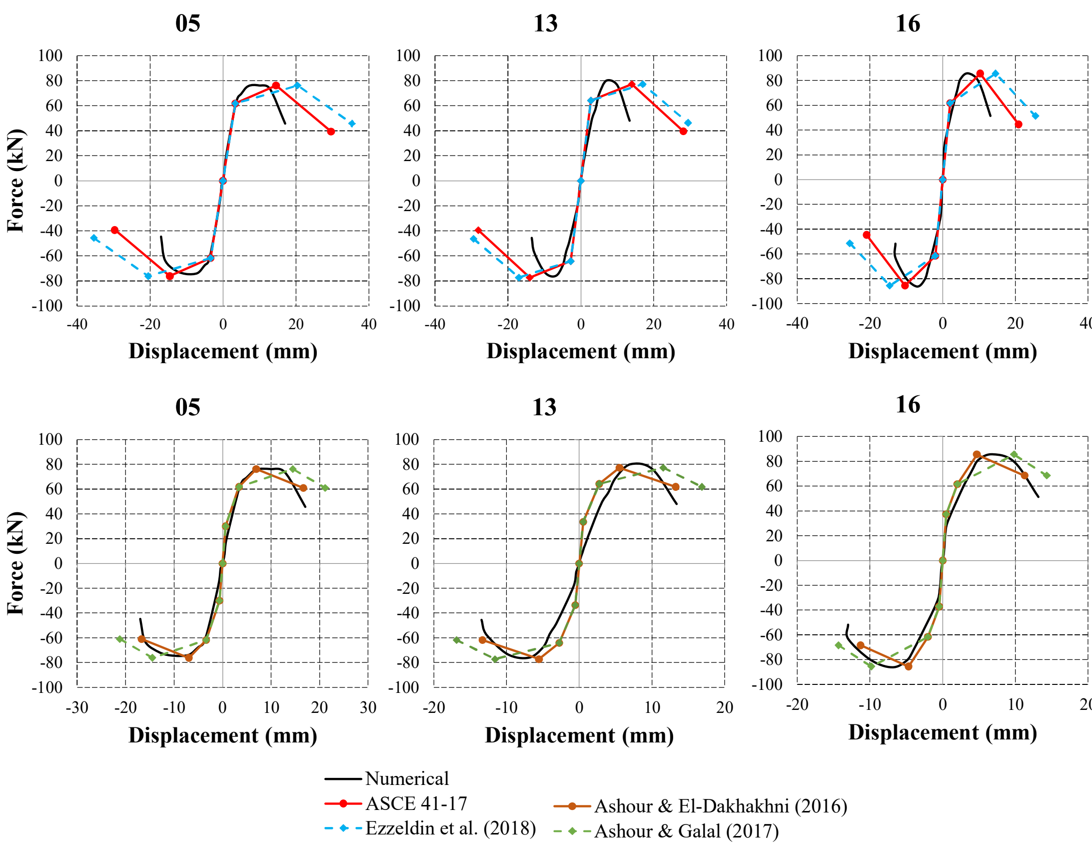

Figure 3: Evaluation of Previous Analytical Models for PG Walls

Parameters of Proposed Model

This section describes the development of a load-displacement backbone model that can predict shear-dominated PG masonry shear response walls. Five key-points define the proposed model: cracking, yielding, ultimate, 20% strength degradation, and 40% strength degradation. The fifth point is considered to account for the post-peak negative stiffness in the force-displacement relationship of PG masonry walls. The shear-dominated walls are characterized by the masonry shear strength, V_m, and nominal shear capacity, V_n, of the walls as presented by Eqs. (1) and (2) [18].

$$V_m = 0.16\left(2 - \frac{M_f}{V_f\, d_v}\right)\sqrt{f'_{m,eff}} \tag{1}$$

$$V_n = \left(V_m\, b_w\, d_v + 0.25 P_d\right)\gamma_g + \left(0.60 A_v\, f_y \frac{d_v}{s}\right) \tag{2}$$

Masonry shear strength, V_m, and nominal shear capacity, V_n, were considered to be the yielding and ultimate capacities, Q_y and Q_u, respectively. Furthermore, using the materials properties, the cracking, M_{cr}, moment can be calculated, and then its corresponding capacity, Q_{cr}, is determined. Finally, the strength of the fourth, $Q_{0.8u}$, and fifth, $Q_{0.6u}$, points are determined as 80% and 60% of the ultimate strength, respectively.

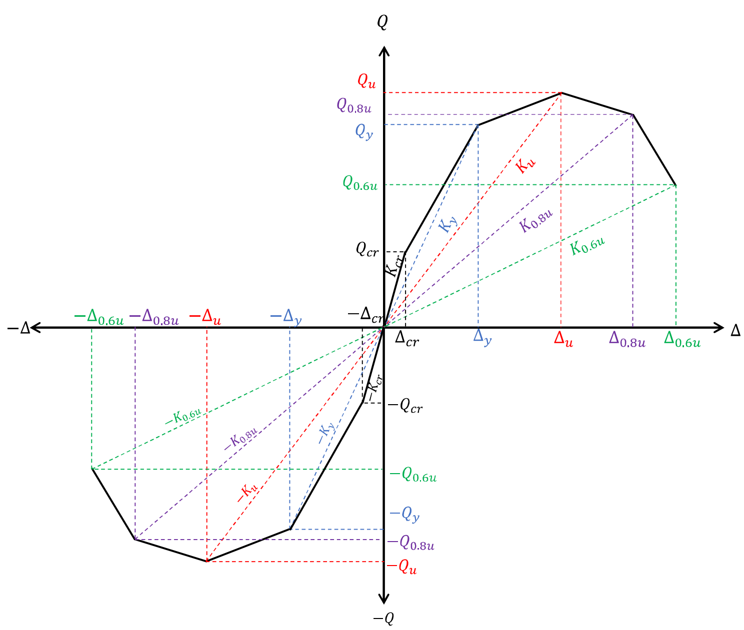

Figure 4: Proposed Backbone Model for PG Walls

The corresponding displacements to the five key points were determined by laying out the values of the performance points on the envelopes of the numerical models. Once the displacements are obtained, the secant stiffnesses of the points are calculated from Hooke's law, as shown in Eq. (3)

and presented by Figure 4. Finally, regression analyses were carried out to relate the stiffnesses obtained from the numerical models and the theoretical gross stiffness, K_g, calculated by Eq. (4).

$$K_i = \frac{Q_i}{\Delta_i} \tag{3}$$

$$K_g = \frac{1}{\dfrac{h_w^{\;3}}{3\,E_{m,eff}\,I_g} + \dfrac{1.2\,h_w}{G_{m,eff}\,A_g}} \tag{4}$$

RESULTS AND DISCUSSION

Stiffness Expressions for Proposed Model

To establish simplified expressions for stiffnesses, the linear type of regression analysis with a non-zero interceptor, to improve the coefficient of determination, was employed in the present study. Moreover, both directions (push and pull) of the numerical models were considered to account for the opposite-directional response and introduce the walls' averaged stiffnesses. This also doubled the density of the data, which would lead to more statistically confident results. 10% of the walls were arbitrarily chosen and excluded from the analyses to be blindly tested against the developed analytical model including one sample of the experimental specimens by Maleki [16] (six numerical and one experimental samples).

As shown in Table 2, the cracking and yielding stiffnesses of shear-dominated PG walls were found to be 33.4% and 25% of the gross stiffness, K_g, with intercepts of 2.865 and 3.249, respectively. The higher interceptors demonstrate that the expressions are notably shifted due to data accumulation at higher values. The ultimate stiffness was 62.3% of that of K_y with a negative intercept of -2.056. The increase in the slope and the negative interceptor would produce lower displacements at the ultimate capacity as anticipated in shear-dominated walls. On the contrary, post-peak points experienced slightly lower slopes of 46.5% and 21.7% with intercepts of 1.115 and 1.409, respectively. Regarding the R-squared, the walls recorded acceptable values for the five points of 84.6%, 90.9%, 83.5%, 92%, and 90.6%, respectively, as shown in Figure 5.

Table 2: Stiffness Expressions for Proposed Model

Point	**Stiffness expression**
Cracking	$K_{cr} = 0.334\,K_g + 2.865$
Yielding	$K_y = 0.250\,K_g + 3.249$
Ultimate	$K_u = 0.623\,K_y - 2.056$
20% degradation	$K_{0.8u} = 0.465\,K_u + 1.115$
40% degradation	$K_{0.6u} = 0.217\,K_u + 1.409$

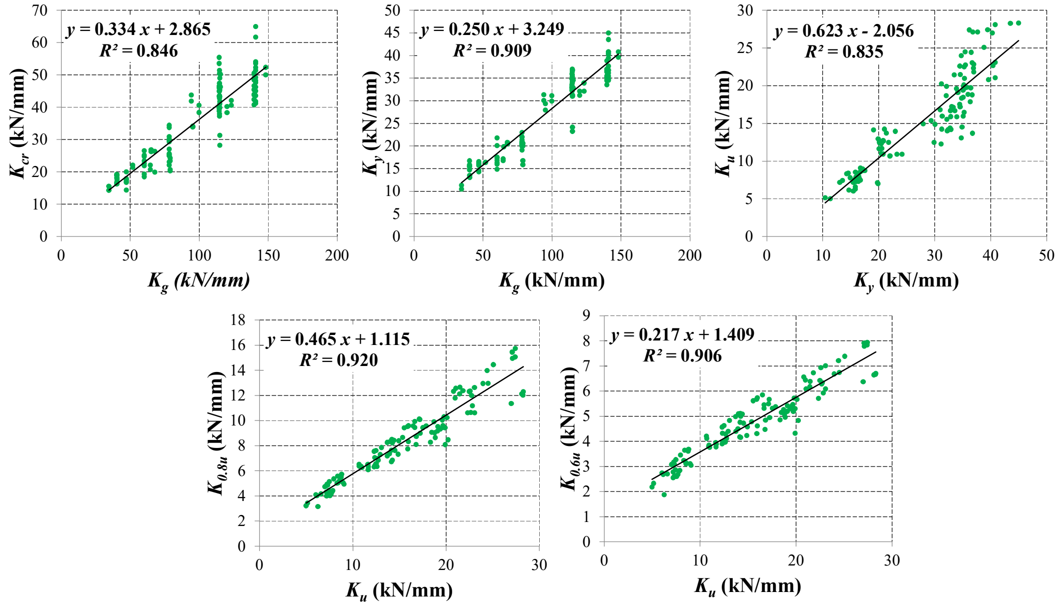

Figure 5: Regression Analysis of Stiffnesses for Shear-Dominated PG Walls

Validation of the Proposed Model Against Selected Samples

Figure 6 presents the numerical envelopes of the randomly selected samples (walls 34, 41, and 51) with proposed quint-linear model. As can be seen, the proposed model can accurately predict the response of shear-dominated PG masonry walls. Unlike the available analytical models in the literature, the model could estimate the initial stiffness, and the yielding and ultimate displacements. In addition, the displacements of the post-peak points were reasonably anticipated. Furthermore, the cracking point was demonstrated to be essential to adjust the initial stiffness.

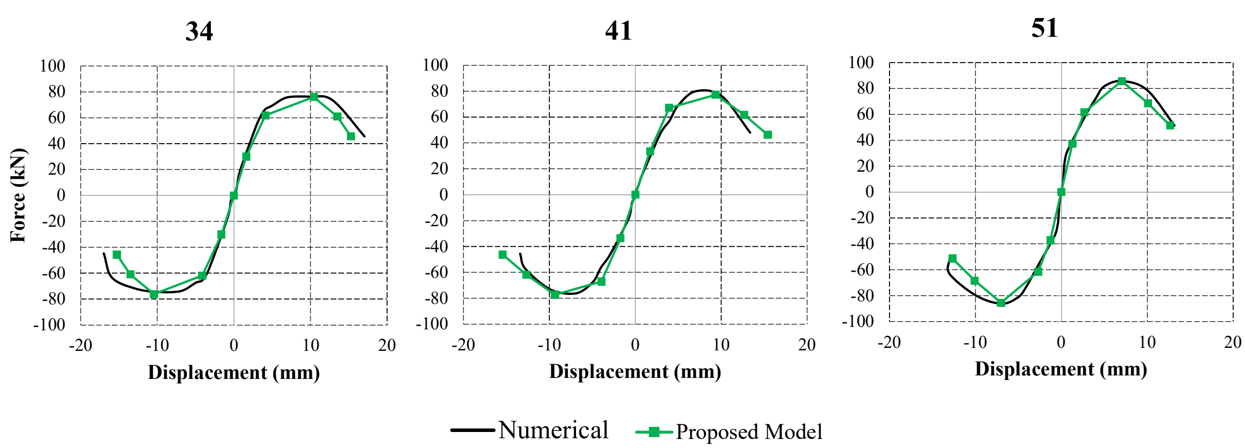

Figure 6: Validation of the Proposed Model Against Selected Samples

Validation of the Proposed Model Against Excluded Samples

As indicated above, 10% of the total walls were arbitrarily excluded for validating the developed model. These walls included six numerical and one experimental specimens (walls 02, 04, 14, 28, 35, 60, and Wall-2). As illustrated by Figure 7, the developed model is capable of capturing the behaviour of shear-dominated PG masonry walls. The initial stiffness, the yielding and ultimate displacements, and the post-peak response were well-predicted. It is worth mentioning that the walls with relatively high flexural capacities showed higher ultimate capacities than the theoretically expected values (increase of 4.6% and 7.4% for wall 14 and wall 60, respectively), as shown in Figure 7.

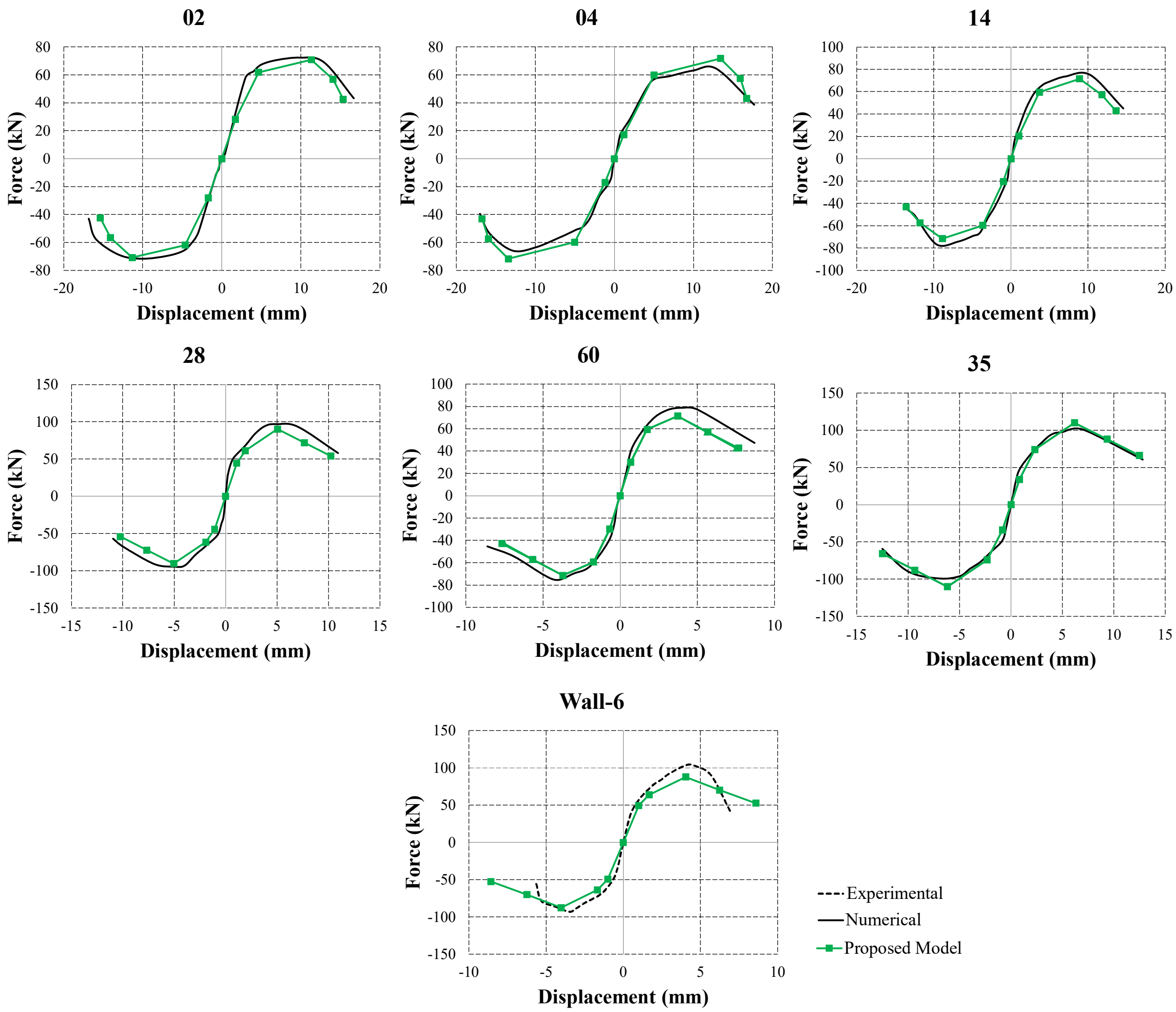

Figure 7: Validation of the Proposed Model Against Excluded Samples

CONCLUSION

In this paper, a 2D simplified-micro model using ABAQUS/Explicit has been generated and validated against experimental data in the literature. Consequently, this FE model was utilized to establish a matrix of 62 numerical models extrapolated from three experimental specimens to cover a wide range of parameters. A brief evaluation of the available analytical models in the literature, [9,11,12,17], was introduced to demonstrate that there is a need to develop simplified analytical models that predict the behaviour of PG masonry shear walls. Therefore, a quint-linear backbone load-displacement model was developed using regression analysis. Finally, five stiffness-based expressions were derived for shear-dominated PG masonry walls that relate the secant stiffnesses of the five performance points. The results showed that the wall's stiffness at cracking point is only about one third of the expected stiffness (gross stiffness), which is a significant finding to account for during the design of PG walls. Moreover, the results demonstrated that the yielding stiffness of PG walls is much lower than that estimated by design standards (i.e. CSA), with a maximum value of 25% of K_g. On the other hand, the ultimate stiffness was found to be in a reasonable range compared to the previous models, Ashour and El-Dakhakhni [9], with a value of 62.3% of K_y for shear-dominated walls. Although, the post-peak stiffnesses showed relative fluctuation that reflect the nature of PG walls' behaviour beyond peak capacity, they reasonably predicted the behaviour with stiffnesses of 46.5% and 21.7% of K_u for $K_{0.8u}$ and $K_{0.6u}$, respectively. These outputs are essential to be considered in design standards as the current provisions are overestimating PG masonry shear walls.

ACKNOWLEDGMENTS

The authors acknowledge support from the Natural Sciences and Engineering Research Council of Canada (NSERC), the Canadian Concrete Masonry Producers Association (CCMPA), and Canada Masonry Design Centre (CMDC).

REFERENCES

[1] Astroza M, Moroni O, Brzev S, Tanner J. Seismic performance of engineered masonry buildings in the 2010 Maule earthquake. Earthq Spectra 2012;28:385–406. https://doi.org/1-0.1193/1.4000040.

[2] Valdebenito G, Alvarado D, Sandoval C, Aguilar V. TERREMOTO DE IQUIQUE Mw=8,2 - 01 ABRIL 2014: DAÑOS OBSERVADOS Y EFECTOS DE SITIO EN ESTRUCTURAS DE ALBAÑILERÍA. XI Congr. Chil. Sismol. e Ing. Sísmica 922 ACHISINA. 18-20 March, Santiago, Chile: 2015.

[3] Bolhassani M, Hamid AA, Moon FL. Enhancement of lateral in-plane capacity of partially grouted concrete masonry shear walls. Eng Struct 2016;108:59–76. https://doi.org/10.1016-/j.engstruct.2015.11.017.

[4] Bolhassani M, Hamid AA, Johnson C, Moon FL, Schultz AE. New Design Detail to Enhance the Seismic Performance of Ordinary Reinforced Partially Grouted Masonry Structures. J Struct Eng (United States) 2016;142:1–15. https://doi.org/10.1061/(ASCE)ST-.1943-541X.0001620.

[5] Bolhassani M. Improvement of Seismic Performance of Ordinary Reinforced Partially Grouted Concrete Masonry Shear Walls. Ph.D Thesis, Drexel University, 2015.

[6] Johnson CA, Schultz AE. Simulated seismic testing of partially-grouted masonry subassem-blages. NCEE 2014 - 10th US Natl Conf Earthq Eng Front Earthq Eng 2014. https://doi.org-/10.4231/D3HX15R69.

[7] Schultz AE, Johnson CA. Seismic resistance mechanisms in partially grouted shear walls with new design details. 13th North Am. Mason. Conf. Mason. Soc., Salt Lake City, UT, USA: 2019.

[8] Ashour A, El-Dakhakhni W, Shedid M. Experimental Evaluation of the System-Level

Seismic Performance and Robustness of an Asymmetrical Reinforced Concrete Block Building. J Struct Eng 2016;142:04016072. https://doi.org/10.1061/(asce)st.1943-541x.0001529.
[9] Ashour A, El-Dakhakhni W. Backbone model for displacement-based seismic design of reinforced masonry shear wall buildings. Brick Block Mason Trends, Innov Challenges - Proc 16th Int Brick Block Mason Conf IBMAC 2016 2016:65–70. https://doi.org/10.1201/b21889-6.
[10] Ashour A, El-Dakhakhni W. Influence of Floor Diaphragm–Wall Coupling on the System-Level Seismic Performance of an Asymmetrical Reinforced Concrete Block Building. J Struct Eng 2016;142:04016071. https://doi.org/10.1061/(asce)st.1943-541x.0001540.
[11] Ezzeldin M, El-Dakhakhni W, Wiebe L. Reinforced Masonry Building Seismic Response Models for ASCE/SEI-41. J Struct Eng 2018;144:04017175. https://doi.org/10.1061/(asce)st.1943-541x.0001914.
[12] Ashour A, Galal K. Load-Displacement Backbone Model for Flexure-Dominated Reinforced Masonry Shear Walls. 13TH Can. Mason. Symp., Halifax, Canada: 2017.
[13] Lourenco P. Computational Strategy for Masonry Structures. 1996.
[14] Hsu LS, Hsu C-TT. Complete stress — strain behaviour of high-strength concrete under compression. Mag Concr Res 1994;46:301–12. https://doi.org/10.1680/macr.1994.46.169.301.
[15] Ewing RD, El-Mustapha AM, Karlotis JC. Fem/I A Finite Element Computer Program for The Nonlinear Static Analysis of Reinforced Masonry Building Components. vol. 53. 1990. https://doi.org/10.1017/CBO9781107415324.004.
[16] Maleki M. Behaviour of partially grouted masonry shear walls under cyclic reversed loading. Ph.D Thesis, McMaster University, 2008.
[17] ASCE/SEI. ASCE standard, ASCE/SEI, 41-17, seismic evaluation and retrofit of existing buildings. Reston, VA: American Society of Civil Engineers; 2017. https://doi.org/10.1061/9780784414859.
[18] Canadian Standard Association. CSA S304-14, Design of Masonry Structures. Mississauga, Ontario, Canada: 2014.